

# Prevalent role of the insulin receptor isoform A in the regulation of hepatic glycogen metabolism in hepatocytes and in mice

Sabela Diaz-Castroverde<sup>1,2,3</sup> · Selene Baos<sup>1</sup> · María Luque<sup>1</sup> · Marianna Di Scala<sup>4</sup> · Gloria González-Asequinolaza<sup>4</sup> · Almudena Gómez-Hernández<sup>1,3</sup> · Nuria Beneit<sup>1</sup> · Oscar Escribano<sup>1,2,3</sup> · Manuel Benito<sup>1,2,3</sup>

Received: 21 December 2015 / Accepted: 8 August 2016 / Published online: 7 September 2016  
© Springer-Verlag Berlin Heidelberg 2016

## Abstract

**Aims/hypothesis** In the postprandial state, the liver regulates glucose homeostasis by glucose uptake and conversion to glycogen and lipids. Glucose and insulin signalling finely regulate glycogen synthesis through several mechanisms. Glucose uptake in hepatocytes is favoured by the insulin receptor isoform A (IRA), rather than isoform B (IRB). Thus, we hypothesised that, in hepatocytes, IRA would increase glycogen synthesis by promoting glucose uptake and glycogen storage.

**Methods** We addressed the role of insulin receptor isoforms on glycogen metabolism in vitro in immortalised neonatal hepatocytes. In vivo, IRA or IRB were specifically expressed in the liver using adeno-associated virus vectors in inducible liver insulin receptor knockout (iLIRKO) mice, a model of type 2 diabetes. The role of IR isoforms in glycogen synthesis and storage in iLIRKO was subsequently investigated.

**Results** In immortalised hepatocytes, IRA, but not IRB expression induced an increase in insulin signalling that was associated with elevated glycogen synthesis, glycogen synthase activity and glycogen storage. Similarly, elevated IRA, but not IRB expression in the livers of iLIRKO mice induced an increase in glycogen content.

**Conclusions/interpretation** We provide new insight into the role of IRA in the regulation of glycogen metabolism in cultured hepatocytes and in the livers of a mouse model of type 2 diabetes. Our data strongly suggest that IRA is more efficient than IRB at promoting glycogen synthesis and storage. Therefore, we suggest that IRA expression in the liver could provide an interesting therapeutic approach for the regulation of hepatic glucose content and glycogen storage.

**Keywords** Adeno-associated viruses · Glucose intolerance · Glycogen metabolism · Insulin receptor isoforms · Liver · Type 2 diabetes mellitus

Oscar Escribano and Manuel Benito contributed equally to this study.

**Electronic supplementary material** The online version of this article (doi:10.1007/s00125-016-4088-z) contains peer-reviewed but unedited supplementary material, which is available to authorised users.

✉ Oscar Escribano  
oescriba@ucm.es

<sup>1</sup> Department of Biochemistry and Molecular Biology II, School of Pharmacy, Complutense University of Madrid, Madrid 28040, Spain

<sup>2</sup> Mechanisms of Insulin Resistance (MOIR) Consortium, Comunidad de Madrid, Madrid, Spain

<sup>3</sup> Centro de Investigación Biomédica en Red de Diabetes y Enfermedades Metabólicas Asociadas (CIBERDEM), Health Institute Carlos III (ISCIII), Spain  
<http://www.ciberdem.org/>

<sup>4</sup> Division of Hepatology and Gene Therapy, Center for Applied Medical Research, University of Navarra, Pamplona, Navarra, Spain

## Abbreviations

AAV	Adeno-associated virus
Alb	Albumin
G6P	Glucose-6-phosphate
GCK	Glucokinase
GSK3	Glycogen synthase kinase 3
GYS2	Liver glycogen synthase
IGF-IR	IGF type I receptor
iLIRKO	Inducible liver insulin receptor knockout
IR	Insulin receptor
IRA	Insulin receptor isoform A
IRB	Insulin receptor isoform B
IRloxP	Mouse hepatocyte expressing IR
IRKO	IR knockout
MAPK	Mitogen-activated protein kinases

PKB	Protein kinase B
PP1	Glycogen synthase phosphatase
PYGL	Liver glycogen phosphorylase

## Introduction

The liver plays a central role in maintaining blood glucose homeostasis by glucose uptake and conversion to glycogen in the postprandial state [1]. Malfunction of the mechanisms by which glucose and insulin regulate glycogen metabolism is a major cause of type 2 diabetes mellitus, the most common metabolic disorder worldwide [2].

The insulin receptor (IR) is a member of the tyrosine kinase receptor superfamily with an essential role in glucose metabolism [3, 4]. The IR is closely related to other receptors such as the IGF type I receptor (IGF-IR) that is involved in normal growth and development [4]. In mammals, alternative splicing gives rise to two isoforms of IR: IRA and IRB. IRB has 12 additional amino acids encoded by exon 11 [5]. This sequence is located immediately downstream of the ligand binding domain but does not affect insulin binding affinity [5, 6]. Moreover, IRA is predominantly expressed during fetal development where it enhances the effects of IGF-II [7]. Conversely, IRB is the predominant IR in adult tissues, including the liver, where it triggers the metabolic effects of insulin [8].

The conversion of glucose into glycogen is a key pathway by which the liver removes glucose in the postprandial state [9]. The most commonly documented signalling pathway for glycogen synthesis is triggered by insulin, which initiates a cascade of events that activate protein kinase B/Akt (PKB/Akt). PKB phosphorylates Ser21 of glycogen synthase kinase 3  $\alpha$  (GSK3 $\alpha$ ) and Ser9 of GSK3 $\beta$ , inactivating GSK3 [10, 11]. GSK3 functions by phosphorylating four out of nine regulatory serine residues (Ser641, Ser645, Ser649, Ser653) on liver glycogen synthase (GYS2). These residues play a critical role in inhibiting GYS2 activity and hence glycogen synthesis [12]. In addition to reversible phosphorylation by GSK3, GYS2 activity is controlled by the allosteric activator, glucose-6-phosphate (G6P) [12]. G6P binding to GYS2 has composite effects in controlling glycogen synthesis through allosteric activation and efficient dephosphorylation, coupled with appropriate cellular localisation [1, 13].

Although insulin does not stimulate hepatic glucose uptake, *in vitro* studies in neonatal hepatocytes demonstrate that IRA plays a direct role in favouring glucose uptake by promoting its specific association with endogenous GLUT1 and GLUT2 [14]. Therefore, differences in glucose uptake can be associated with the presence/absence of IR isoforms or with changes in their ratio. However, the functional significance of each IR isoform in glycogen synthesis currently remains unclear.

Based on *in vitro* studies that have demonstrated a close relationship between IRA and GLUT1/GLUT2 [14], we hypothesised that this association may play a key role in regulating hepatic glycogen synthesis in adult hepatocytes. In the current study, we demonstrate the differential roles of IR isoforms in the regulation of glycogen metabolism by employing two different approaches: *in vitro* investigation using neonatal hepatocytes and *in vivo* studies of inducible liver insulin receptor knockout (iLIRKO) mice, a model of type 2 diabetes in which IRA or IRB were expressed specifically in the liver.

## Methods

**Hepatocyte cell line generation and genotyping** Mouse immortalised hepatocytes expressing IR (IRloxP), lacking IR (IRKO) and exclusively expressing IRA or IRB were previously generated and characterised in our laboratory [14]. Hepatocytes were genotyped by RT-PCR; RNA was prepared using Trizol (Life Technologies, Carlsbad, CA, USA), cDNA was synthesised using a high capacity reaction kit (Applied Biosystems, Foster City, CA, USA) and PCR was performed with DNA AmpliGel Master Mix (Biotools, Jupiter, FL, USA). The primers used to determine exon 4 deletion were 5'-CTGTTCTCGGAACCTGATGAC-3' and 5'-ATAC CAGAGCATAGGAG-3'. Primers flanking the human exon 11 were 5'-AGGAAGACGTTTGAGGATT-3' and 5'-CACC GTCACATTCCCAACAT-3'. A 316 bp band and a 280 bp band correspond to IRB and IRA, respectively. The cells were mycoplasma free and checked for contamination by PCR every month.

**Cell culture** Cell lines were grown in 10 cm Petri dishes in DMEM (25 mmol/l glucose, pH 7.4) supplemented with 10% FBS (vol./vol.), penicillin (12  $\mu$ g/ml), streptomycin (10  $\mu$ g/ml), amphotericin (10  $\mu$ g/ml) and MycoZap™ (500 $\times$ ) (Lonza, Allendale, NJ, USA), until they reached 80–90% confluence. In each passage, cells were divided by trypsinisation (Invitrogen, Madrid, Spain). For signalling experiments, cells were starved for 6 h with serum-free, low-glucose DMEM (5 mmol/l glucose, pH 7.4) supplemented with 0.2% BSA (wt/vol.) (Sigma-Aldrich, St Louis, MO, USA). The hepatocytes were then stimulated with insulin (Sigma-Aldrich) at various doses (0.1–100 nmol/l).

**Mice and diets** IR<sup>(lox/lox)</sup> mice were created by homologous recombination using an IR gene targeting vector with loxP sites flanking exon 4 [15]; these mice were a generous gift from R. Kahn (Joslin Diabetes Center, Boston, MA, USA). For liver-specific deletions we used transgenic mice expressing tamoxifen-dependent Cre-ER<sup>T2</sup> recombinase under the control of albumin promoter (Alb-Cre-ER<sup>T2</sup>) that were kindly provided by the P. Chambon laboratory

(IGBMC, Ilkirch, France) [16]. The iLIRKO mice were generated by crossing C57Bl/6-IR<sup>(lox/lox)</sup> with heterozygous C57Bl/6-Alb-Cre-ER<sup>T2</sup>, whilst littermates IR<sup>(lox/lox)</sup> mice were used as controls. Genotyping of IR<sup>(lox/lox)</sup> and Alb-Cre-ER<sup>T2</sup> transgenic mice was performed by PCR using genomic DNA isolated from the tail tip of 4-week-old mice, as previously described [16]. After weaning, iLIRKO and IR<sup>(lox/lox)</sup> mice were fed on a soy-free diet (RMS-0909-US-EN-02-DS-2016, Harlan, Indianapolis, IN, USA) for 2 weeks followed by 2 weeks of a tamoxifen diet (TD.09327, Harlan, Indianapolis, IN, USA) to induce Cre translocation to the nucleus [16]. Animals were then fed standard chow ad libitum. Only male animals were used in the study. Animals were maintained on a 12 h light–dark cycle. All animal experimentation described in this article was conducted in accordance with accepted standards of animal use as approved by the Complutense University of Madrid Committee.

**Metabolic tests** Blood glucose levels were measured 30 min after i.p. glucose administration (2 g/kg body weight) in 16 h overnight fasted mice. The measurements were performed using Accu-Check blood glucose strips and a glucometer (Roche, Penzberg, Germany).

#### Viral constructs and vector production and purification

Recombinant adeno-associated virus (AAV) vectors were constructed with a transgene cassette coding sequence for the individual spliced isoforms of the *INSR* single chain. The transgene cassette was flanked by AAV2 (serotype 2) wild-type inverted terminal repeats. rAAV8 (serotype 8) vectors were produced as previously described [17]. Viral titres were determined by qPCR and were performed three times in triplicate at three different dilutions.

**AAV administration** AAVs were administered via i.v. injection to 5-month-old mice. For all procedures, animals were anaesthetised by i.p. injection of a mixture of xylazine (Rompun 2% (wt/vol.), Bayer, Leverkusen, Germany) and ketamine (Imalgene 50, Merial, Lyon, France), 1:9 vol./vol. Four months post-AAV administration, the mice were euthanised for further analysis.

**Western blot** Cell homogenates were obtained from cell monolayers scraped with lysis buffer [18] and tissues were homogenised, as previously described [15]. Protein quantification was performed using the Bradford method [19]. Western blot analysis of insulin signalling proteins was carried out using liver homogenates as previously described [18]; antibodies against IGF-I (H-70; 1:500), IGF-II (H-103; 1:500), GLUT2 (H-67; 1:500), IR $\beta$  (C:19; 1:1000), IGF-IR $\beta$  (C:20; 1:500) and glucokinase (GCK; H-88; 1:500) were purchased from Santa Cruz Biotechnology (Dallas, TX, USA). GLUT1 (1:500) was purchased from Chemicon

(Billerica, MA, USA) and  $\beta$ -Actin (1:10,000) from Sigma-Aldrich. PKB and p-PKB (Ser473), p44/p42 mitogen-activated protein kinases (MAPK) and p-p44/p42 MAPK (Thr202/Tyr204), p70S6 kinase and p-p70S6 kinase (Thr389), GSK3 $\alpha/\beta$  (D75D3) and p-GSK3 $\alpha/\beta$  (Ser21/9), and glycogen synthase 2 (GYS2; 15B1) were all from Cell Signaling (Danvers, MA, USA) and used at a 1:1000 dilution. Phosphotyrosine (4G10), IRS1 and phospho-GYS2 (Ser641/Ser645) were all from Millipore (Billerica, MA, USA) and used at 1:500. Liver glycogen phosphorylase (PYGL; 1:1000) was purchased from Acris Antibodies (Herford, Germany), whilst p-PYGL (Ser14; 1:1000) was provided by the Division of Signal Transduction Therapy, University of Dundee (Dundee, Scotland, UK). All antibodies were raised in rabbit, other than  $\beta$ -actin and phosphotyrosine antibodies which were raised in mouse. Primary antibodies were immunodetected using horseradish peroxidase-conjugated polyclonal antibodies from sheep (GE Healthcare, Buckingham, England, UK). Antibodies were used in strict accordance with the manufacturer's instructions as described in datasheets. The band intensities were quantified using ImageJ (<http://rsb.info.nih.gov/ij>).

**Glycogen content determination** Cells ( $2.2 \times 10^6$ ) were seeded in 10 cm dishes in DMEM (25 mmol/l glucose) supplemented with 10% FBS (vol./vol.). When 70–80% confluence was reached, cells were serum-starved for 6 h in DMEM (5 mmol/l glucose) supplemented with 0.2% BSA (wt/vol.). The medium was then changed to high-glucose DMEM (25 mmol/l glucose) and cells were stimulated with different doses of insulin (10–100 nmol/l). Cell monolayers were frozen after 6 h of incubation and scraped in 30% KOH (wt/vol.). Glycogen was precipitated when the homogenates were transferred onto Whatman 3MM (Sigma-Aldrich) paper with 66% ethanol (vol./vol.) at  $-20^\circ\text{C}$ , as previously described [20]. Precipitated glycogen was released in the form of glucose monomers via incubation with 1.6 mg/ml of  $\alpha$ -amylglucosidase (Sigma-Aldrich) for 4 h at  $37^\circ\text{C}$ , in 0.4 mol/l acetate buffer (pH 4.8). Glucose was measured at 500 nm using a Biosystems kit (Barcelona, Spain).

Similarly, *in vivo*, livers were obtained from mice that were euthanised following a 24 h fast and a 1 h refeeding period. Twenty-five mg of liver tissue was homogenised with 30% KOH (wt/vol.), heated at  $100^\circ\text{C}$  and glycogen content was determined as in cultured cells.

**Glycogen synthesis analysis** Cells ( $8 \times 10^5$ ) were plated in 6 cm dishes in DMEM (25 mmol/l glucose) supplemented with 10% FBS (vol./vol.). At 70–80% confluence, cells were starved for 6 h in serum-free DMEM (5 mmol/l glucose) with 0.2% BSA (wt/vol.). At the moment of stimulation with 10 or 100 nmol/l insulin, the medium was changed to DMEM (25 mmol/l glucose) with 10 mmol/l of [ $U$ - $^{14}\text{C}$ ]glucose (11.1 GBq/ $\mu\text{mol}$ ; PerkinElmer, Waltham, MA, USA), as

previously described [20]. After glycogen precipitation using ice-cold 66% ethanol (vol./vol.), Whatman papers were dried using a heater set at 40°C. The radioactivity was quantified using a  $\beta$ -radiation counter (LKB Wallac-Rackbeta Counter; Abbott Laboratories, Libertyville Township, IL, USA).

**Determination of glycogen synthase and glycogen phosphorylase enzymatic activities** Glycogen synthase activity was estimated in all cell lines by the incorporation of UDP[U- $^{14}$ C]glucose in the presence of 10 nmol/l insulin, as previously described [1]. Glycogen phosphorylase activity was also measured in cells using a spectrophotometric assay, as described by Company et al, in the presence of 5.5 mmol/l glucose [21].

**Statistical analysis** Data are presented as means  $\pm$  SEM from at least three independent experiments. In the in vivo experiments, we used at least four mice. Differences between two groups were assessed using unpaired two-tailed *t* tests. Data involving more than two groups were assessed by ANOVA followed by Bonferroni tests, unless otherwise specified. A *p* value of <0.05 was considered to be statistically significant. No data were excluded from the statistical analysis. The experimenters were blind to group assignment and outcome assessment.

## Results

Since the IR is the gatekeeper of the insulin signalling pathway, we assessed the impact of IR deletion or reconstitution with IRA or IRB on several molecules in the insulin signalling cascade, under basal conditions. The deletion of IR in IRKO hepatocytes was confirmed by western blot (Fig. 1a). The *Insr* exon 4 deletion was also detected by RT-PCR in mRNA from IRloxP and IRKO hepatocytes (Fig. 1b). Moreover, hepatocytes bearing IRA or IRB were found to express the corresponding *INSR* isoform at an mRNA level (Fig. 1c).

From western blot analyses, it was also found that IRKO and IRB hepatocytes expressed significantly higher levels of IGF-IR, as compared with IRloxP or IRA hepatocytes. In contrast, IGF-I levels were significantly lower in IRKO cells compared with IRloxP, although no changes were observed in IRA or IRB hepatocytes. GSK levels were significantly increased in IRA and significantly decreased in IRB cells, when compared with IRloxP hepatocytes, whilst GYS2 levels were significantly higher in IRB than in IRloxP and IRA cells. Additionally, p70S6K expression levels were significantly increased in IRKO, IRA and IRB hepatocytes compared with IRloxP cells. IRS1 expression was significantly lower in IRKO than in IRloxP cells, whilst its expression in IRB was significantly higher than in all other cell types. Our results also revealed a significant decrease in IRS2 levels in IRB cells, compared with IRloxP and IRA hepatocytes. Finally, there

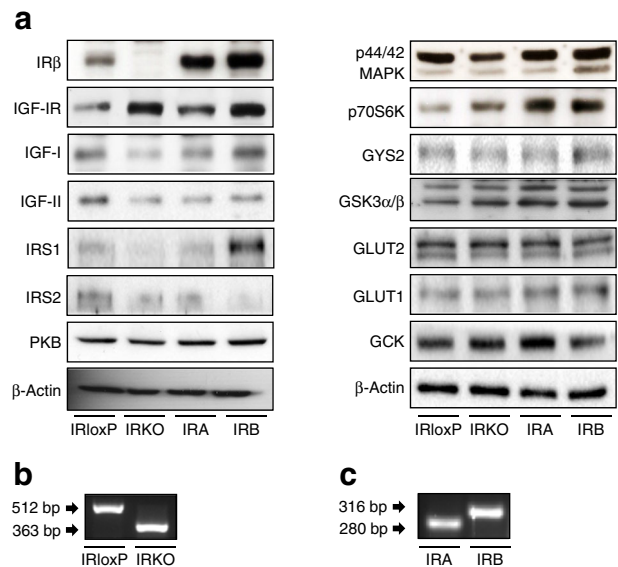


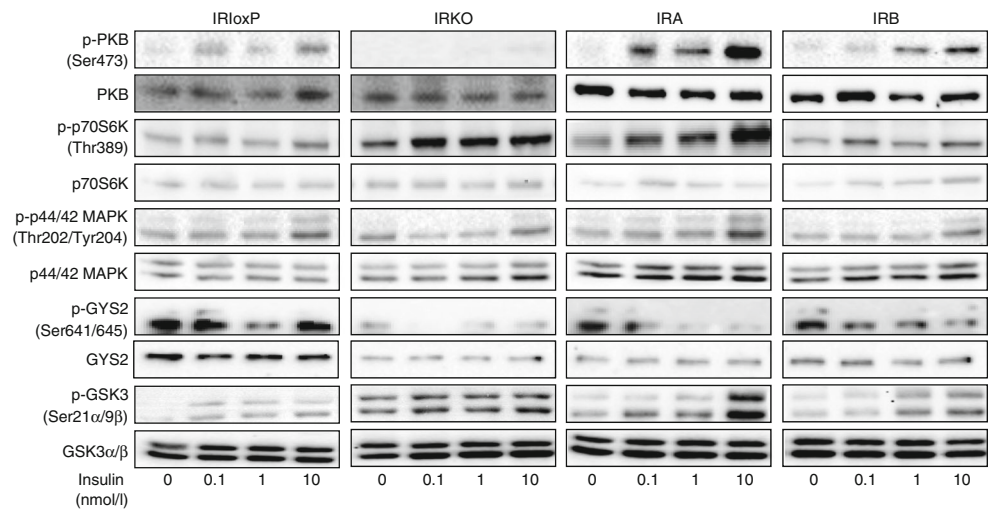
**Fig. 1** Characterisation of the hepatocyte cell lines. (a) The main proteins in the insulin signalling pathway were analysed by western blot in IRloxP, IRKO, IRA and IRB hepatocytes ( $n=4$ ).  $\beta$ -Actin was used as a loading control. (b) Total RNA was isolated and *Insr* exon 4 deletion was measured by RT-PCR in IRloxP and IRKO hepatocytes ( $n=4$ ). (c) *INSR* isoforms were analysed in IRA and IRB hepatocytes determining exon 11 deletion by RT-PCR ( $n=4$ )

were no significant differences in IGF-II, PKB, p44/42 MAPK, GSK3 $\alpha$ / $\beta$ , GLUT1 and GLUT2 levels (Fig. 1a and ESM Fig. 1).

To address the issue of the differential role of IR isoforms in hepatic glucose metabolism, we focused our studies on the insulin response of glycogen metabolism in several hepatocyte cell lines. The two major pathways employed by IR isoforms include MAPKs and PKB/Akt. Significant phosphorylation of PKB in IRloxP cells was observed after 10 nmol/l insulin stimulation, whereas IRKO cells did not respond to insulin. Interestingly, PKB activation in IRA hepatocytes was much greater compared with IRB cells (Fig. 2).

In addition, IRKO cells showed higher activation of p70S6K compared with IRloxP hepatocytes. In the case of IR isoforms, IRA hepatocytes presented higher p70S6K activation than IRB cells at all the insulin doses assayed. p44/42 MAPK phosphorylation was significantly higher in IRloxP cells at 10 nmol/l insulin, compared with basal conditions, but once again p44/42 MAPK was less activated in IRB-expressing hepatocytes than in IRA cells. Insulin-stimulated GSK3 $\alpha$ / $\beta$  phosphorylation was higher in IRA hepatocytes than in the other cell lines treated with 10 nmol/l insulin. Additionally, by use of a phosphospecific antibody against the GSK3 $\alpha$ / $\beta$  phosphorylation sites of GYS2 (Ser641/Ser645), we found that GYS2 was unexpectedly less phosphorylated in IRKO cells than in IRloxP cells, suggesting that IRKO cells are more prone to glycogen synthesis. Furthermore, we found that, in response to insulin, GYS2

**Fig. 2** Enhanced insulin signalling in IRA vs IRB neonatal hepatocytes. Dose–response effect of insulin (0–10 nmol/l) on PKB, p70S6K, p44/42 MAPK, GYS2 and GSK3 $\alpha/\beta$  phosphorylation in IRloxP, IRKO, IRA and IRB hepatocytes. Cells were starved of serum for 5 h and then stimulated with insulin (0–10 nmol/l) for 5 min. Cells were lysed and analysed by western blot ( $n=6$ ). Total PKB, p70S6K, p44/42 MAPK, GYS2 and GSK3 $\alpha/\beta$  were used as loading controls



was less phosphorylated in IRA vs IRB cells, treated under the same conditions (Fig. 2 and ESM Fig. 2).

Glycogen synthesis was significantly increased in IRKO cells compared with IRloxP cells under basal conditions. This finding is in agreement with the GYS2 dephosphorylation status described above (Fig. 2 and Fig. 3a). However, despite this increment, differences in glycogen content did not reach significance relative to IRloxP hepatocytes (Fig. 3b). This result can be explained by the significant

increase observed in PYGL phosphorylation status and activity in IRKO cells (Fig. 3d, e). Together, these results suggest an increase in glycogen synthesis and degradation in the absence of the IR.

Moreover, glycogen synthesis and content in IRA cells was significantly higher than in other cells assayed, probably due to a significant increase in GYS2 activity (Fig. 3a–c). However, similar findings were not observed in IRB cells (Fig. 3a). Glycogen synthesis and content following 6 h of

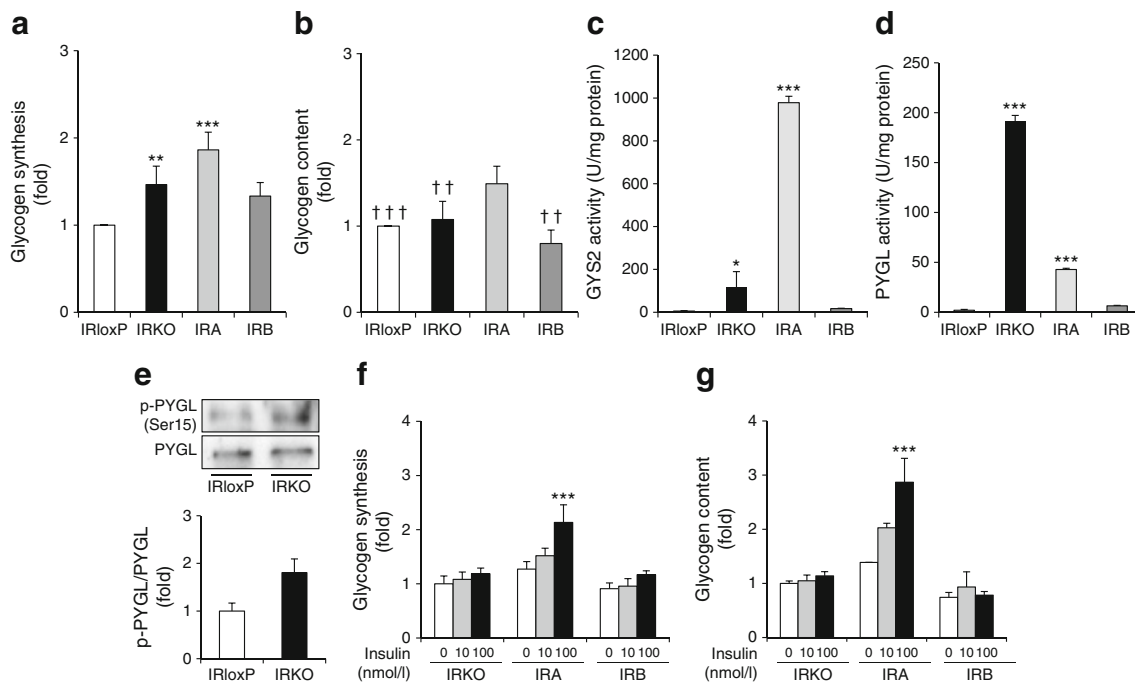


**Fig. 3** Differential enzyme regulation and glycogen accumulation by IR isoforms (IRloxP, IRKO, IRA and IRB) in hepatocytes. Measurement of (a) glycogen synthesis and (b) glycogen content was performed under basal conditions. (c) GYS2 enzymatic activity was measured in the presence of 10 nmol/l insulin. (d) PYGL enzymatic activity was measured in the presence of 5.5 mmol/l glucose. (a–d) \* $p < 0.05$ , \*\* $p < 0.01$ , \*\*\* $p < 0.001$  vs IRloxP; †† $p < 0.01$ , ††† $p < 0.001$  vs IRA;  $t$  test. Data are

means  $\pm$  SEM ( $n=4$ ). (e) Effect of 5.5 mmol/l glucose in serum-starved cells on PYGL phosphorylation in IRloxP and IRKO hepatocytes. PYGL was used as a loading control. Histograms show quantification of band intensities. Measurement of (f) glycogen synthesis and (g) glycogen content in IRKO, IRA and IRB hepatocytes stimulated with insulin (10 or 100 nmol/l) for 6 h. (f, g) \*\*\* $p < 0.001$  vs IRA basal condition; ANOVA. Data are means  $\pm$  SEM ( $n=4$ )

insulin stimulation at 100 nmol/l were significantly elevated in IRA hepatocytes, compared with IRKO and IRB cells (Fig. 3f, g). In agreement with the insulin dose–response data, GYS2 dephosphorylation occurred in both IRA and IRB hepatocytes following 100 nmol/l insulin stimulation for 5 min. However, lower levels of GSK3 $\alpha/\beta$  and PYGL phosphorylation were observed in IRB hepatocytes in comparison with IRA cells under basal conditions or when stimulated with 100 nmol/l insulin (Fig. 4a), suggesting that, compared with IRA cells, IRB cells have an altered glycogen turnover.

In addition to phosphorylation, liver GYS2 is controlled by the allosteric activator, G6P. Previous work has demonstrated that changes in the expression of proteins in the insulin signalling pathway are dependent on glucose levels [1, 22]. To dissect the roles of glucose and insulin on GYS2 activation, we analysed the effects of different doses of glucose in IRA or IRB hepatocytes in the absence of insulin. Although total levels of GSK3 $\alpha/\beta$  were the same in IRA and IRB hepatocytes, GSK3 $\alpha$  phosphorylation was absent in IRB cells. Consistent with this finding, GYS2 was less phosphorylated in IRA hepatocytes in the absence of glucose than in IRB hepatocytes. Nevertheless, in a high-glucose medium (25 mmol/l), IRA and IRB hepatocytes showed similar levels of phosphorylated GYS2 (Fig. 4b).

Impaired storage and utilisation of glucose are major contributors to the pathophysiology of diabetes. Therefore, we addressed the physiological relevance of the differential effect

of IRA vs IRB on the regulation of glycogen metabolism in the livers of iLIRKO mice. These animals present targeted disruption of IR and markedly impaired glucose tolerance and insulin secretion (Fig. 5a–c). To reconstitute IR expression in iLIRKO mice, we developed recombinant AAV vectors that expressed IRA or IRB under the control of a liver-specific promoter ( $\alpha$ -1-antitrypsin). In 20-week-old diabetic mice, the specific hepatic expression of IRA, but not IRB, ameliorated hyperglycaemia and hyperinsulinaemia (Fig. 5a–c), and decreased beta cell hyperplasia/hypertrophy, reversing the diabetic phenotype approximately 8 weeks after viral administration (data not shown). After 24 h starvation followed by 1 h refeeding, iLIRKO mice showed slightly decreased glycogen content compared with control mice. However, iLIRKO IRA mice exhibited significantly elevated glycogen content in comparison with controls or iLIRKO mice under the same experimental conditions. Because the distribution of IR isoforms in the livers of adult mice favours IRB rather than IRA, the glycogen content found in iLIRKO IRB mice is similar to control mice (Fig. 5d). Analysis of the glycogen synthesis pathway confirmed that iLIRKO IRA mice had lower GYS2 levels compared with iLIRKO IRB mice, however, the p-GYS2/GYS2 ratio was similar. Finally, GSK3 $\alpha/\beta$  phosphorylation was significantly lower in livers of iLIRKO IRB mice, compared with iLIRKO IRA mice (Fig. 5e). Despite the limited effect of IRB on glycogen content, its expression in vivo was completely functional in

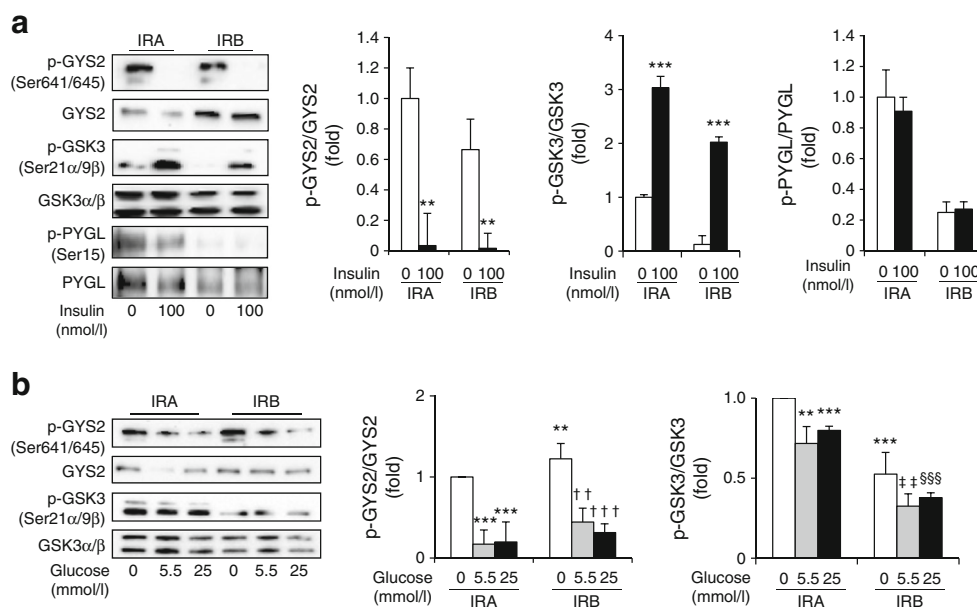


**Fig. 4** Glycogen synthesis in response to glucose is more highly favoured in IRA hepatocytes than IRB cells in vitro. **(a)** Effect of insulin on GYS2, GSK3 $\alpha/\beta$  and PYGL phosphorylation in IRA and IRB hepatocytes. Cells were starved of serum in a 0.1 g/l glucose-containing medium for 5 h and then stimulated with 100 nmol/l insulin for 5 min. GYS2, GSK3 $\alpha/\beta$  and PYGL were used as loading controls. Histograms show quantification of band intensities. Data are means  $\pm$  SEM ( $n = 5$ ). \*\* $p < 0.01$ , \*\*\* $p < 0.001$  vs basal conditions. **(b)** Effect

of glucose on GYS2 and GSK3 $\alpha/\beta$  phosphorylation in IRA and IRB hepatocytes. Cells were starved of serum in 5.5 and 25 mmol/l glucose-containing medium for 5 h. GYS2 and GSK3 $\alpha/\beta$  were used as loading controls. Histograms show quantification of band intensities. Data are means  $\pm$  SEM ( $n = 5$ ). \*\* $p < 0.01$ , \*\*\* $p < 0.001$  vs IRA basal conditions; †† $p < 0.01$ , ††† $p < 0.001$  vs IRB basal condition; ††† $p < 0.01$  vs IRA 5.5 mmol/l glucose; §§§ $p < 0.001$  vs IRA 25 mmol/l glucose

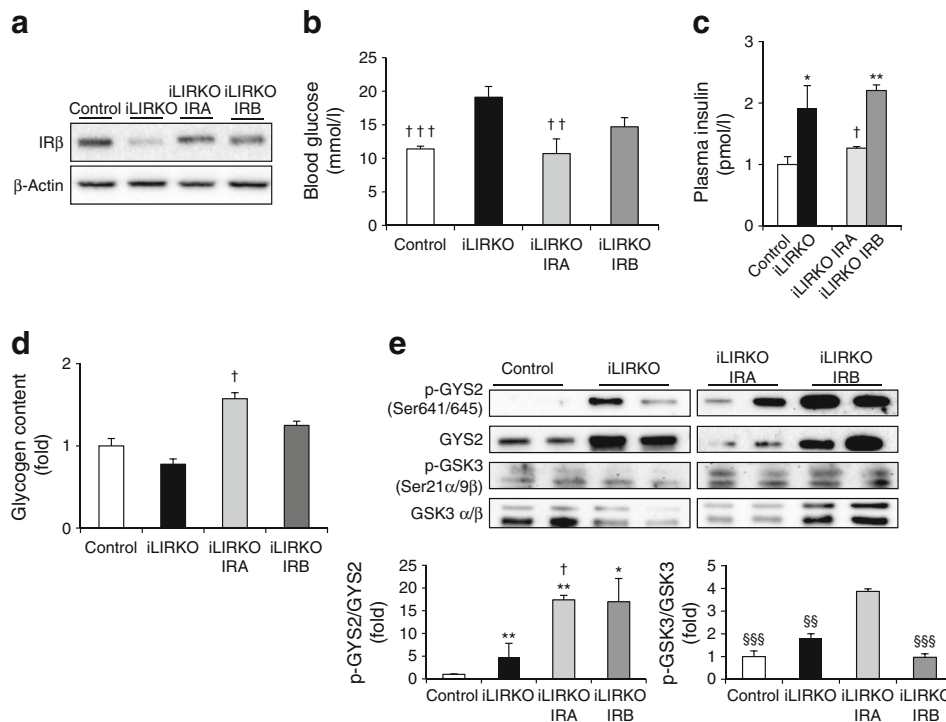


**Fig. 5** Differential regulation of glycogen metabolism and glucose homeostasis by IR isoforms in diabetic iLIRKO mice. **(a)** IR $\beta$  subunit levels were analysed by western blot in liver homogenates obtained from 5-month-old control and iLIRKO mice ( $n = 10$ ).  $\beta$ -Actin was used as a loading control. **(b)** Blood glucose levels were measured 30 min after glucose injection (2 g/kg body weight) in Control, iLIRKO, iLIRKO IRA and iLIRKO IRB mice ( $n = 4$ –10 animals per group).  $\dagger\dagger p < 0.01$ ,  $\dagger\dagger\dagger p < 0.001$  vs iLIRKO. **(c)** Plasma insulin levels were measured in 16 h fasted control and iLIRKO mice immediately prior to AAV administration. In iLIRKO IRA and iLIRKO IRB mice, insulin levels were determined under the same conditions, 4 months after AAV treatment

( $n = 10$ ).  $*p < 0.05$ ,  $**p < 0.01$  vs Control. **(d)** Glycogen content was measured in Control, iLIRKO, iLIRKO IRA, iLIRKO IRB mice after 24 h fasting and 1 h refeed ( $n = 4$ ).  $\dagger p < 0.05$  vs iLIRKO. **(e)** Liver lysates from mice after 24 h fasting and 1 h refeed were immunoblotted using p-GYS2 and p-GSK3 antibodies; results from two different mice per genotype are shown. GYS2 and GSK3 $\alpha/\beta$  were used as loading controls. Data are means  $\pm$  SEM for each experimental group. Representative immunoblots of four independent experiments are shown. Histograms show quantification of band intensities.  $*p < 0.05$ ,  $**p < 0.01$  vs Control;  $\dagger p < 0.05$  vs iLIRKO;  $\S\S p < 0.01$ ,  $\S\S\S p < 0.001$  vs iLIRKO IRA

response to insulin in terms of downstream signalling, as shown in ESM Fig. 3 (see ESM Methods for details).

## Discussion

The importance of glucose in controlling hepatic glycogen synthesis and glucose homeostasis is well established. In the postprandial state, insulin drives the conversion of glucose to glycogen, replenishing glycogen stores in the liver and suppressing glucose output [1]. An increase in blood glucose concentration is a prerequisite for hepatic glycogen synthesis, which stimulates insulin secretion and subsequent activation of PKB, which in turn inhibits GSK3 $\alpha/\beta$ , a negative regulator of GYS2 [1, 9, 23]. IR isoforms have been linked to differential insulin signalling in beta cells [2, 24]; IRA is involved in insulin signalling leading to insulin gene transcription, whereas IRB signals through PKB leading to GSK3 $\alpha/\beta$  expression [2]. The roles of the IR isoforms were investigated using: (1) immortalised neonatal IRloxP and IRKO hepatocytes and those exclusively expressing

IRA or IRB in vitro; and (2) in vivo studies in iLIRKO mice, a model of type 2 diabetes, specifically expressing IRA or IRB in the liver.

Our in vitro results suggest a strong correlation between enhanced insulin signalling and increased glycogen synthesis and storage in response to insulin in IRA hepatocytes, when compared with IRB cells. This effect may be reinforced by the increased glucose uptake/transport observed in IRA hepatocytes vs IRB cells [14]. The liver possesses glucose-sensing components; there are several enzymes and regulatory proteins involved in the regulation of hepatic glycogen synthesis [9, 25]. Stimulation of GLUT2 expression by glucose in cultured hepatocytes results from the activation of gene transcription and requires active glucose metabolism. The metabolites responsible for this effect have not yet been identified but are downstream of G6P formation. Moreover, an increase in cellular G6P is known to induce a conformational change in glycogen synthase, making it a better substrate for dephosphorylation (activation) by glycogen synthase phosphatase (PP1) [1, 9]. Activation of GYS2 by PP1 is inhibited by phosphorylated PYGL, but this inhibition is abolished by elevated

glucose concentrations [26]. Consistent with this, G6P also regulates GYS2 activity by allosteric activation, even when it is hyperphosphorylated [1, 27]. Hence, because of the higher expression of GCK and, consequently, GYS2 activity in IRA cells, not only is glucose uptake increased, but intracellular glucose disposal is also favoured. Contrastingly, the opposite was found in IRB hepatocytes, where both glucose uptake and GCK expression were significantly decreased.

Compared with IRloxP cells, increased glycogen synthesis in IRKO hepatocytes was found to correlate with higher GSK3 $\alpha/\beta$  inhibition under basal conditions. In contrast, remarkable activation of PYGL (a direct product of glycogen degradation) in IRKO cells, may explain their lack of significant glycogen storage. These findings suggest a futile glycogen synthesis/glycogen depletion cycle which may compensate for the loss of glucose input due to the absence of IRs.

In vivo, the lack of hepatic IR appears to destabilise the balance between glucose utilisation and production by the liver. The final outcome is a diabetic phenotype showing a severe compensatory hyperinsulinaemia, accompanied by postprandial and fasting hyperglycaemia [28, 29]. These data strongly suggest that the IR alone is involved in both glucose disposal and glucose output by the liver. Therefore, we hypothesise that a shift in the IRA/IRB ratio might result in a substantial change in hepatic glucose consumption and glycogen storage. Glycogen content in iLIRKO IRA mice was significantly increased compared with control mice, probably due to enhanced glucose uptake, increasing its availability for glycogen synthesis in these mice. Although these results cannot be explained by variation in GYS2 dephosphorylation (activation) in iLIRKO IRA vs iLIRKO IRB mice, our results suggest that differential G6P availability might play a major role in the regulation of GYS2 activation, as previously described [1, 13].

In conclusion, our results highlight the central and complex role that hepatic IR isoforms play in the control of hepatic glucose metabolism. We provide in vitro and in vivo evidence that hepatic IRA is more efficient than IRB at increasing glycogen synthesis, glycogen synthase activity and glycogen storage in hepatocytes. Our results suggest that the specific expression of IRA, but not IRB, in the liver could be an important therapeutic approach for the regulation of hepatic glucose consumption and glycogen storage.

**Acknowledgements** The authors want to thank to C. R. Kahn (Joslin Diabetes Center, Boston, MA, USA) for the gift of the human insulin receptor sequences.

#### Compliance with ethical standards

**Funding** This work was supported by grants SAF2011/22555 and SAF2014/51795-R from Ministerio de Ciencia e Innovación, Comunidad de Madrid (S2010/BMD-2423). CIBERDEM is an ISCIII project (PIE14/00061).

**Duality of interest** The authors declare that there is no duality of interest associated with this manuscript.

**Contribution statement** SD-C participated in the experimental design, acquisition, analysis and interpretation of data, and drafted the paper. SB, ML, MDS, GG-A, AG-H and NB participated in the acquisition, analysis and interpretation of data, and critically revised the manuscript. OE participated in the experimental design, analysis and interpretation of data, and wrote the manuscript. MB participated in the design of the study and wrote the manuscript. All authors drafted the article, revised it critically for important intellectual content and approved the final manuscript. OE and MB are the guarantors of this work.

## References

1. von Wilamowitz-Moellendorff A, Hunter RW, García-Rocha M et al (2013) Glucose-6-phosphate-mediated activation of liver glycogen synthase plays a key role in hepatic glycogen synthesis. *Diabetes* 62:4070–4082
2. Leibiger B, Leibiger IB, Moede T et al (2001) Selective insulin signaling through A and B insulin receptors regulates transcription of insulin and glucokinase genes in pancreatic beta cells. *Mol Cell* 7:559–570
3. Benyoucef S, Surinya KH, Hadaschik D, Siddle K (2007) Characterization of insulin/IGF hybrid receptors: contributions of the insulin receptor L2 and Fn1 domains and the alternatively spliced exon 11 sequence to ligand binding and receptor activation. *Biochem J* 403:603–613
4. Ward CW, Lawrence MC (2009) Ligand-induced activation of the insulin receptor: a multi-step process involving structural changes in both the ligand and the receptor. *Bioessays* 31:422–434
5. Whittaker J, Sørensen H, Gadsbøll VL, Hinrichsen J (2002) Comparison of the functional insulin binding epitopes of the A and B isoforms of the insulin receptor. *J Biol Chem* 277:47380–47384
6. Menting JG, Whittaker J, Margetts MB et al (2013) How insulin engages its primary binding site on the insulin receptor. *Nature* 493:241–245
7. Frasca F, Pandini G, Scalia P et al (1999) Insulin receptor isoform A, a newly recognized, high-affinity insulin-like growth factor II receptor in fetal and cancer cells. *Mol Cell Biol* 19:3278–3288
8. Malaguamera R, Belfiore A (2011) The insulin receptor: a new target for cancer therapy. *Front Endocrinol (Lausanne)* 2:1–16
9. Agius L (2008) Glucokinase and molecular aspects of liver glycogen metabolism. *Biochem J* 414:1–18
10. Frame S, Cohen P, Biondi RM (2001) A common phosphate binding site explains the unique substrate specificity of GSK3 and its inactivation by phosphorylation. *Mol Cell* 7:1321–1327
11. MacAulay K, Doble BW, Patel S et al (2007) Glycogen synthase kinase 3 $\alpha$ -specific regulation of murine hepatic glycogen metabolism. *Cell Metab* 6:329–337
12. Roach PJ, Depaoli-Roach AA, Hurley TD, Tagliabracci VS (2012) Glycogen and its metabolism: some new developments and old themes. *Biochem J* 441:763–787
13. Gomis RR, Favre C, García-Rocha M, Fernández-Novell JM, Ferrer JC, Guinovart JJ (2003) Glucose 6-phosphate produced by gluconeogenesis and by glucokinase is equally effective in activating hepatic glycogen synthase. *J Biol Chem* 278:9740–9746
14. Nevado C, Valverde AM, Benito M (2006) Role of insulin receptor in the regulation of glucose uptake in neonatal hepatocytes. *Endocrinology* 147:3709–3718



15. Brüning JC, Michael MD, Winnay JN et al (1998) A muscle-specific insulin receptor knockout exhibits features of the metabolic syndrome of NIDDM without altering glucose tolerance. *Mol Cell* 2:559–569
16. Schuler M, Dierich A, Chambon P, Metzger D (2004) Efficient temporally controlled targeted somatic mutagenesis in hepatocytes of the mouse. *Genesis* 39:167–172
17. Gil-Fariña I, Di Scala M, Vanrell L et al (2013) IL12-mediated liver inflammation reduces the formation of AAV transcriptionally active forms but has no effect over pre-existing AAV transgene expression. *PLoS One* 8:e67748
18. Valverde AM, Lorenzo M, Pons S, White MF, Benito M (1998) IRS-1 and IRS2 differential signaling in the insulin/IGF-1 pathways in fetal brown adipocytes. *Mol Endocrinol* 12:688–697
19. Bradford NM (1976) A rapid and sensitive method for the quantitation of microgram quantities of protein utilizing the principle of protein-dye binding. *Anal Biochem* 72:248–254
20. Alonso-Chamorro M, Nieto-Vazquez I, Montori-Grau M, Gomez-Foix AM, Fernandez-Veledo S, Lorenzo M (2011) New emerging role of protein-tyrosine phosphatase 1B in the regulation of glycogen metabolism in basal and TNF- $\alpha$ -induced insulin-resistant conditions in an immortalized muscle cell line isolated from mice. *Diabetologia* 54:1157–1168
21. Company M, Zuluaga J, Jimenez JS (1988) Continuous spectrophotometric assay for glycogen phosphorylase activity. *Int J Biol Macromol* 10:21–25
22. Rencurel F, Waeber G, Antoine B et al (1996) Requirement of glucose metabolism for regulation of glucose transporter type 2 (GLUT2) gene expression in liver. *Biochem J* 314:903–909
23. Frame S, Cohen P (2001) GSK3 takes centre stage more than 20 years after its discovery. *Biochem J* 359:1–16
24. Escribano O, Gómez-Hernández A, Díaz-Castroverde S et al (2015) Insulin receptor isoform A confers a higher proliferative capability to pancreatic beta cells enabling glucose availability and IGF-I signaling. *Mol Cell Endocrinol* 5:82–91
25. Burkhardt BR, Parker MJ, Zhang YC, Song S, Wasserfall CH, Atkinson MA (2005) Glucose transporter-2 (GLUT2) promoter mediated transgenic insulin production reduces hyperglycemia in diabetic mice. *FEBS Lett* 579:5759–5764
26. Bollen M, Keppens S, Stalmans W (1998) Specific features of glycogen metabolism in the liver. *Biochem J* 336:19–31
27. Stalmans W, Cadefau J, Wera S, Bollen M (1997) New insight into the regulation of liver glycogen metabolism by glucose. *Biochem Soc Trans* 25:19–25
28. Michael MD, Kulkarni RN, Postic C et al (2000) Loss of insulin signaling in hepatocytes leads to severe insulin resistance and progressive hepatic dysfunction. *Mol Cell* 6:87–97
29. Escribano O, Guillén C, Nevado C, Gómez-Hernández A, Kahn CR, Benito M (2009) Beta-Cell hyperplasia induced by hepatic insulin resistance: role of a liver-pancreas endocrine axis through insulin receptor A isoform. *Diabetes* 58:820–828